Concept study of a novel energy harvesting-enabled tuned mass-damper-inerter (EH-TMDI) device for vibration control of harmonically-excited structures

Jonathan Salvi*, Agathoklis Giaralis

Department of Civil Engineering, City University of London,
Northampton Square, London EC1V 0HB, UK

E-mail: jonathan.salvi@city.ac.uk (*Contact Author),
agathoklis.giaralis.1@city.ac.uk

Abstract. A novel dynamic vibration absorber (DVA) configuration is introduced for simultaneous vibration suppression and energy harvesting from oscillations typically exhibited by large-scale low-frequency engineering structures and structural components. The proposed configuration, termed energy harvesting-enabled tuned mass-damper-inerter (EH-TMDI) comprises a mass grounded via an in-series electromagnetic motor (energy harvester)-inerter layout, and attached to the primary structure through linear spring and damper in parallel connection. The governing equations of motion are derived and solved in the frequency domain, for the case of harmonically-excited primary structures, here modelled as damped single-degree-of-freedom (SDOF) systems. Comprehensive parametric analyses proved that by varying the mass amplification property of the grounded inerter, and by adjusting the stiffness and the damping coefficients using simple optimum tuning formulae, enhanced vibration suppression (in terms of primary structure peak displacement) and energy harvesting (in terms of relative velocity at the terminals of the energy harvester) may be achieved concurrently and at near-resonance frequencies, for a fixed attached mass. Hence, the proposed EH-TMDI allows for relaxing the trade-off between vibration control and energy harvesting purposes, and renders a dual-objective optimisation a practically-feasible, reliable task.

1. Introduction

The concept of the linear tuned mass-damper (TMD) is historically one of the first and most widely used strategies for passive vibration mitigation of harmonically-excited mechanical and civil engineering structures [1–3]. It relies on attaching an additional free-to-vibrate mass to a primary or host structure, whose motion is to be suppressed, via a linear spring/stiffener in parallel with a dashpot (e.g., a linear viscous damper). Spring and dashpot coefficients are appropriately designed (or "tuned") for an *a-priori* specified attached mass and primary structure such that a resonant out-of-phase motion of the attached mass is achieved compared to that of the primary structure. This allows for significant kinetic energy to be transferred from the primary structure to the attached mass, and eventually dissipated by the dashpot in the form of heat (e.g. [4–8]).

The potential of the TMD to harvest energy from large-amplitude low-frequency oscillating primary structures has been recently recognised and explored by several researchers (e.g. [9–14]). It relies on the idea of replacing (or complementing) the dashpot of the TMD with

either electromagnetic devices/motors, for relatively large-scale applications (e.g. [9–13]), or piezoelectric materials, for relatively small-scale applications (e.g. [12, 14]), which are able to transform part of the kinetic energy of the primary structure into electric energy via appropriate energy harvesting and storage circuitry [13,15]. In this context, a tuned mass-damper/harvester (TMD/H) control configuration is proposed in [13], where an electromagnetic motor consisted of a magnet travelling within a constant magnetic field was considered, along with a linear spring and a damper, to link the attached mass to the primary structure. Along similar lines, an electromagnetic transducer connected to an energy harvesting-enabled circuit is used to transform kinetic energy into electric power and to provide controlled force vibrations mitigation for TMD-equipped multi-storey buildings structures in [11]. Further, an energy harvester-dynamic vibration absorber (EH-DVA) configuration is employed in [14], in which electric energy is generated from strains developed in layers of piezoelectric material mounted onto the attached vibrating mass of a TMD.

No matter the scale of the application and the technology used to harvest energy from TMD equipped harmonically-excited structures, it is well documented in the literature through analytical, numerical, and experimental work that energy harvesting and vibration suppression are, in principle, conflicting objectives at least for devices under passive mode of operation [13, 14]. Therefore, there is a design trade-off between the above objectives which depends heavily on the attached TMD mass.

Aiming to solve this issue, this paper proposes a novel configuration for simultaneous vibration suppression and energy harvesting for harmonically-excited structures, modelled as damped single-degree-of-freedom (SDOF) dynamic systems in which the available amount of energy to be harvested and the achieved level of vibration suppression as evaluated in the mechanical domain (i.e., without explicitly considering the dynamics introduced by the energy harvesting and electric storage circuitry) do not have an inverse proportional relationship. The proposed configuration, termed energy harvesting-enabled tuned mass-damper-inerter (EH-TMDI), couples the classical TMD with: (a) an electromagnetic motor (EM), which may work as an energy harvester, and (b) an inerter device [16], in a sky-hook configuration. In this manner, the apparent inertia of the TMD and the relative velocity between the terminals of the EM depend on the grounded inerter.

The latter has been conceptually defined by Smith [16] as a linear two-terminal device of negligible mass/weight which resists the relative acceleration of its terminals with a constant of proportionality, the so-called inertance, measured in mass units (kg) and being independent from the physical device mass. In this respect, the herein considered EH-TMDI is mostly related to the works in [17, 18] where dual-mass TMDs are used to achieve enhanced energy harvesting capabilities through dynamic mass amplification using EM devices [17] and piezoelectric material [18]. However, in the EH-TMDI the mass magnification effect comes from the grounded inerter at no additional weight.

The remainder of the paper is organised as follows. In Section 2, the topology of the EH-TMDI for SDOF primary structures is introduced, and dimensionless mechanical parameters characterising the dynamic response of the considered coupled EH-TMDI primary structure system are defined. In Section 3, the governing equations of motion of a harmonically-excited EH-TMDI equipped SDOF primary structure are derived in the time domain along with the frequency response functions. Section 4 discusses in detail the reported results from a comprehensive parametric study undertaken to gauge the influence of the various dimensionless parameters to the achieved level of vibration suppression and available energy to be harvested separately by the EH-TMDI. Section 5 provides further analytically-derived data to shed light on the role of the inertance for the performance of the EH-TMDI for simultaneous vibration suppression and energy harvesting. Finally, Section 6 summarises the salient conclusions of the present work.

2. Description and topology of the proposed EH-TMDI configuration

Consider the classical linear TMD of mass m_T shown in Fig. 1a, attached to a linear damped SDOF oscillator via a linear dashpot with damping coefficient c_T and a linear spring of stiffness k_T. The oscillator represents the primary structure whose response to the external dynamic force $F_S(t) = F_0 e^{i\omega t}$ is controlled by the TMD. The primary structure is characterised by the natural frequency ω_S and the damping ratio ζ_S defined by:

$$\omega_S = \sqrt{\frac{k_S}{m_S}}, \quad \zeta_S = \frac{c_S}{2\sqrt{k_S m_S}}. \tag{1}$$

where m_S, k_S, and c_S are the mass, stiffness, and damping coefficients of the SDOF oscillator, respectively.

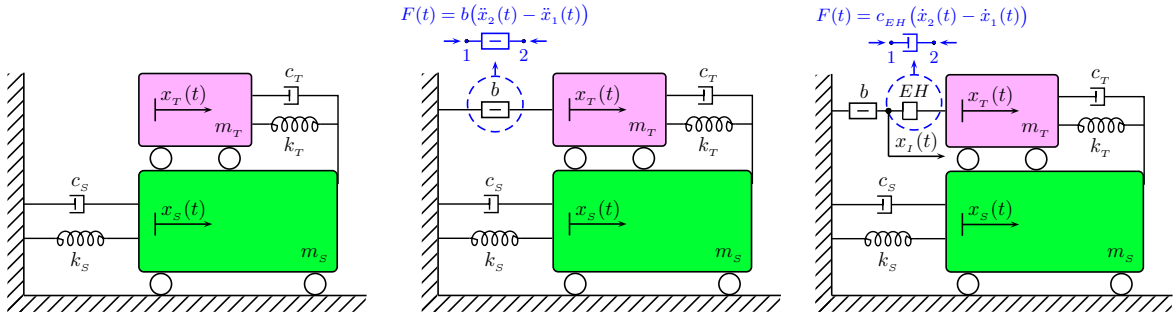

(a) TMD. **(b)** TMDI. **(c)** EH-TMDI.

Figure 1. Structural parameters and absolute (relative to the ground) dynamic degrees of freedom of a structural system composed of a SDOF primary structure (subscript S) equipped with different devices, within a sky-hook layout (subscripts T, I).

The tuned mass-damper-inerter (TMDI) is a generalisation of the classical TMD, introduced by Marian and Giaralis [19, 20] for structural passive vibration control under stochastic broadband (white noise) and narrowband (colored noise) base excitations. For the case of SDOF primary structures, the TMDI incorporates an inerter device connecting the attached mass of a classical TMD to the ground within a sky-hook configuration, as shown in Fig. 1b.

The following relationship holds for a force $F_I(t)$ applied externally to the terminals of an inerter, and being in equilibrium with the resisting force developed internally by the device, as shown in the inlet of Fig. 1b [16]:

$$F_I(t) = b\big(\ddot{x}_2(t) - \ddot{x}_1(t)\big). \tag{2}$$

In the equation above, $x_1(t)$, $x_2(t)$ are the displacement coordinates of the inerter terminals and, hereafter, a dot over a symbol signifies differentiation with respect to time t. Further, the constant of proportionality b is the so-called inertance, which has mass units and fully characterises the behaviour of the ideal inerter. In light of Eq. (2), and by assuming a massless inerter (just as the TMD spring and damper are massless), it is trivial to see that for force excited SDOF primary structures the TMDI with inertance b and attached mass m_T coincides with the classical TMD with attached mass $(m_T + b)$. This consideration motivates the following definitions for the TMDI natural frequency ω_T and damping ratio ζ_T [21]:

$$\omega_T = \sqrt{\frac{k_T}{m_T + b}}, \quad \zeta_T = \frac{c_T}{2\sqrt{k_T(m_T + b)}}. \tag{3}$$

Built on the TMDI concept, this study considers the energy harvesting-enabled tuned mass-damper-inerter (EH-TMDI) configuration shown in Fig. 1c for simultaneous vibration control and energy harvesting from force-induced oscillations of the primary structure. The proposed EH-TMDI incorporates a standard linear electromagnetic motor, similar to those considered in the literature for energy harvesting from large-amplitude low-frequency oscillations [10, 12, 13, 22, 23], connected in series with the inerter and the attached mass of the TMDI ($m_{_T} + b$). The EM contributes a force proportional to the relative velocity of its two terminals to the structural dynamic system in Fig. 1c and, therefore, can be modelled through a dashpot with viscous damping coefficient $c_{_{EH}}$ as shown in the inlet of Fig. 1c [13, 23].

In all ensuing numerical work, the EM damping coefficient is taken as a constant during the excitation (i.e., shunt damping in passive operation mode) [13]. Note that this assumption implies that the EM is not harvesting energy as it is connected to a purely resistant circuit. Still, the above assumption is sufficient for the purposes of this study which aims to evaluate the changes to the vibration suppression performance and to the available energy to be harvested by the EM, for different mechanical properties of the devices comprising the EH-TMDI configuration in Fig. 1c, rather than to quantify the actual amount of energy harvested by the EM. The latter requires probing into the electrical domain of the energy harvester to characterise its operation and, therefore, specifying a particular type of electromagnetic motor, energy harvesting circuitry and energy storage/usage (see e.g. [13, 15]). However, such considerations fall outside the scope of this work. In this regard, the damping ratio $\zeta_{_{EH}}$ associated with the EM is defined as:

$$\zeta_{_{EH}} = \frac{c_{_{EH}}}{2\sqrt{k_{_T}(m_{_T}+b)}}\,, \tag{4}$$

in analogy to the definitions in Eq. (3), by accounting an effective harvesting damping ratio $\zeta_{_{EH,h}}$ and a parasitic (mechanical) damping ratio $\zeta_{_{EH,p}}$, that is, $\zeta_{_{EH}} = \zeta_{_{EH,h}} + \zeta_{_{EH,p}}$ [24]. It is noted in passing that, in establishing the herein proposed EH-TMDI configuration, several alternative topologies involving different connectivity between the inerter, the EM, the TMD spring and damper have been also examined. They were all found less advantageous for the purpose of relaxing the trade-off between energy harvesting and vibration control. One of such alternative topologies, previously considered in the literature [21], is discussed in Section 4 and compared to the above EH-TMDI configuration (Fig. 1c), in view of pertinent analytically-derived results.

3. Governing equations of motion of the proposed EH-TMDI

The equations of motion for the EH-TMDI of Fig. 1c in the time domain read as:

$$\begin{cases} m_{_S}\ddot{x}_{_S}(t) + c_{_S}\dot{x}_{_S}(t) + c_{_T}(\dot{x}_{_S}(t) - \dot{x}_{_T}(t)) + k_{_S}x_{_S}(t) + k_{_T}(x_{_S}(t) - x_{_T}(t)) = F_{_S}(t) \\ m_{_T}\ddot{x}_{_T}(t) + c_{_T}(\dot{x}_{_T}(t) - \dot{x}_{_S}(t)) + k_{_T}(x_{_T}(t) - x_{_S}(t)) + c_{_{EH}}(\dot{x}_{_T}(t) - \dot{x}_{_I}(t)) = 0 \\ c_{_{EH}}(\dot{x}_{_I}(t) - \dot{x}_{_T}(t)) + b\ddot{x}_{_I}(t) = 0 \end{cases}, \tag{5}$$

where $x_{_S}(t)$, $x_{_T}(t)$ and $x_{_I}(t)$ are the displacement coordinates of the primary structure, of the attached mass, and of the node connecting the inerter to the EM, respectively, while null initial conditions assumption applies. By introducing the following non-dimensional parameters, namely the mass ratio μ, the frequency ratio f and the inertance ratio β:

$$\mu = \frac{m_{_T}}{m_{_S}}\,, \quad f = \frac{\omega_{_T}}{\omega_{_S}}\,, \quad \beta = \frac{b}{m_{_S}}\,, \tag{6}$$

and dividing by $(m_{_S}\omega_{_S}^2) = k_{_S}$, the system of Eq. (5) can be written matrix form as:

$$\mathbf{M}\ddot{\mathbf{x}}(t) + \mathbf{C}\dot{\mathbf{x}}(t) + \mathbf{K}\mathbf{x}(t) = \mathbf{F}(t)\,, \tag{7}$$

where $\mathbf{M}$, $\mathbf{C}$ and $\mathbf{K}$ are the non-dimensional mass, damping, and stiffness matrices given as:

$$\mathbf{M} = \begin{bmatrix} 1 & 0 & 0 \\ 0 & \mu & 0 \\ 0 & 0 & \beta \end{bmatrix}$$

$$\mathbf{C} = \begin{bmatrix} 2\zeta_S\omega_S + 2\zeta_T\omega_T(\mu+\beta) & -2\zeta_T\omega_T(\mu+\beta) & 0 \\ -2\zeta_T\omega_T(\mu+\beta) & 2(\zeta_T+\zeta_{EH})\omega_T(\mu+\beta) & -2\zeta_{EH}\omega_T(\mu+\beta) \\ 0 & -2\zeta_{EH}\omega_T(\mu+\beta) & 2\zeta_{EH}\omega_T(\mu+\beta) \end{bmatrix}. \tag{8}$$

$$\mathbf{K} = \begin{bmatrix} \omega_S^2 + \omega_T^2(\mu+\beta) & -\omega_T^2(\mu+\beta) & 0 \\ -\omega_T^2(\mu+\beta) & \omega_T^2(\mu+\beta) & 0 \\ 0 & 0 & 0 \end{bmatrix}$$

Furthermore, in Eq. (7), $\mathbf{F}(t)$ and $\mathbf{x}(t)$ are the force and the displacement vectors, which for harmonic force excitation with frequency ω are written as:

$$\mathbf{F}(t) = \begin{bmatrix} 1 \\ 0 \\ 0 \end{bmatrix} \frac{F_0}{k_S} e^{i\omega t}, \quad \mathbf{x}(t) = \begin{bmatrix} x_S \\ x_T \\ x_I \end{bmatrix} e^{i\omega t}. \tag{9}$$

where i is the imaginary unit. Note that, for the purposes of this study, only the case of force-excited primary structures is discussed. This is because the focus is on relatively small attached masses ($\mu < 5\%$) and, therefore, the analytical results presented in the following sections and pertinent discussions apply also for the case of base-excited primary structures, for which the loading vector takes the form $F(t) = [1,\, \mu,\, 0]^{\mathrm{T}}\omega^2\,(F_0/k_S)e^{i\omega t}$, where the superscript T denotes matrix transposition. The equations of motion in the time domain can be conveniently solved in the frequency domain by Fourier transforming Eq. (7) and solving for the vector $\mathbf{X}(ig) = [X_S(ig), X_T(ig), X_I(ig)]^{\mathrm{T}}$, by collecting the Fourier-transformed elements of the displacement vector $\mathbf{x}(t)$ written in terms of the normalised frequency $g = \omega/\omega_S$:

$$\mathbf{X}(ig) = \mathbf{H}(ig)\mathbf{F}(ig), \tag{10}$$

where $\mathbf{F}(ig)$ is the excitation vector in the frequency domain, and the receptance matrix $\mathbf{H}(ig)$ is written as:

$$\mathbf{H}(ig) = \big[-g^2\mathbf{M} + ig\mathbf{C} + \mathbf{K}\big]^{-1} = \frac{1}{\det\big(-g^2\mathbf{M} + ig\mathbf{C} + \mathbf{K}\big)} \begin{bmatrix} H_{11}(ig) & H_{12}(ig) & H_{13}(ig) \\ H_{21}(ig) & H_{22}(ig) & H_{23}(ig) \\ H_{31}(ig) & H_{32}(ig) & H_{33}(ig) \end{bmatrix}, \tag{11}$$

where:

$$\begin{aligned}
H_{11}(ig) &= [-g^2\mu + ig2(\zeta_T+\zeta_{EH})f(\mu+\beta) + f^2(\mu+\beta)][-g^2\beta + ig2\zeta_{EH}f(\mu+\beta)] + \\
&\quad - [-ig2\zeta_{EH}f(\mu+\beta)]^2 \\
H_{21}(ig) &= (-1)[-ig2\zeta_T f(\mu+\beta) - f^2(\mu+\beta)][-g^2\beta + ig2\zeta_{EH}f(\mu+\beta)] \\
H_{31}(ig) &= [-ig2\zeta_T f(\mu+\beta) - f^2(\mu+\beta)][-ig2\zeta_{EH}f(\mu+\beta)] \\
H_{12}(ig) &= (-1)[-ig2\zeta_T f(\mu+\beta) - f^2(\mu+\beta)][-g^2\beta + ig2\zeta_{EH}f(\mu+\beta)] \\
H_{22}(ig) &= [-g^2 + ig2(\zeta_S + \zeta_T f(\mu+\beta)) + (1 + f^2(\mu+\beta))][-g^2\beta + ig2\zeta_{EH}f(\mu+\beta)], \\
H_{32}(ig) &= (-1)[-g^2 + ig2(\zeta_S + \zeta_T f(\mu+\beta)) + (1 + f^2(\mu+\beta))][-ig2\zeta_{EH}f(\mu+\beta)] \\
H_{13}(ig) &= [-ig2\zeta_T f(\mu+\beta) - f^2(\mu+\beta)][-ig2\zeta_{EH}f(\mu+\beta)] \\
H_{23}(ig) &= (-1)[-g^2 + ig2(\zeta_S + \zeta_T f(\mu+\beta)) + (1 + f^2(\mu+\beta))][-ig2\zeta_{EH}f(\mu+\beta)] \\
H_{33}(ig) &= [-g^2 + ig2(\zeta_S + \zeta_T f(\mu+\beta)) + (1 + f^2(\mu+\beta))][-g^2\mu + \\
&\quad + ig2(\zeta_T+\zeta_{EH})f(\mu+\beta) + f^2(\mu+\beta)] - [-ig2\zeta_T f(\mu+\beta) - f^2(\mu+\beta)]^2
\end{aligned} \tag{12}$$

and the superscript -1 denoting matrix inversion.

4. Parametric analysis for harmonic excitation

In this section, a comprehensive parametric investigation on the dynamic response of the proposed EH-TMDI configuration, added on a damped linear SDOF structures, under harmonic force excitation is undertaken, to assess the potential of the EH-TMDI for simultaneous vibration suppression and energy harvesting. To this aim, the dynamic amplification factor of the displacement response of the primary structure, given by [3, 25]

$$N(g) = \left| \frac{X_S(ig)}{F_0/k_S} \right|, \tag{13}$$

and the available energy to be harvested by the EM within a full cycle of response, given by [24, 25]

$$P_{EH}(g) = \frac{1}{2} c_{EH,h} g^2 \left| \frac{X_T(ig) - X_I(ig)}{F_0/k_S} \right|^2 = \zeta_{EH,h} f(\mu+\beta) g^2 \left| \frac{X_T(ig) - X_I(ig)}{F_0/k_S} \right|^2, \tag{14}$$

are used to gauge the effectiveness of the EH-TMDI to suppress the oscillatory motion of the primary structure and to scavenge energy, respectively, as a function of the normalised excitation frequency $g = \omega/\omega_S$. Specifically, the above defined functions $N(g)$ and $P_{EH}(g)$ are analytically evaluated using the expressions in Eqs. (10)–(12), and plotted in Figs. 2–3, respectively, for different values of the inertance ratio β, the mass ratio μ, the damping ratio of the primary structure ζ_S and the damping ratio introduced by the energy harvester ζ_{EH}. In all considered cases, a parasitic EH damping $\zeta_{EH,p} = 0.01$ is considered, in line with experimental data reported in the literature [10].

Furthermore, the attached mass ratio μ is taken equal to 1%. This choice yields relatively lightweight EH-TMDIs, whose inertial property is leveraged by varying the inertance ratio β.

Moreover, the following expressions are used to tune the frequency ratio f and the damping ratio ζ_T, for given mass ratio μ and primary structure damping ratio ζ_S:

$$f = \frac{1}{1+\mu+\beta}, \quad \zeta_T = \sqrt{\frac{3(\mu+\beta)}{8(1+\mu+\beta)}}. \tag{15}$$

The above formulae can be readily derived using the standard Den Hartog approach [2] for a conventional TMD with mass property $m_T + b$ (i.e., a TMDI with attached mass m_T and inertance b) mounted on a harmonically force-excited undamped SDOF primary structure ($\zeta_S = 0$). It is therefore recognised that these expressions do not yield, by any means, optimum design parameters for the EH-TMDI corresponding to any particular optimisation criterion. They are only adopted to determine reasonable values for the stiffness and the damping properties of the EH-TMDI as a function of the attached mass and inertance in the context of the herein undertaken parametric analysis.

Focusing on the furnished analytical results for the dynamic amplification factor in Eq. (13), it is seen in all panels of Fig. 2 that the considered EH-TMDI reduces significantly the peak response of the primary structure at resonance ($g = 1$) and within a band of $\pm 5\%$ of the resonant normalised excitation frequency g, that is, in a range of values of $g = [0.95,\ 1.05]$. The level of this reduction depends heavily on the damping ratio of the primary structure ζ_S, as well as on the properties of the EH-TMDI considered in the parametric study, namely the inertance ratio and the energy harvester damping ratio. Specifically, it is seen in Fig. 2a that small increases of ζ_S, of the order of 1%, lead to considerable reduction of the peak response of the EH-TMDI equipped primary structure, of the order of 25%, which is instead much less affected by changes to the EM damping ratio as evidenced by comparing Figs. 2a–2b.

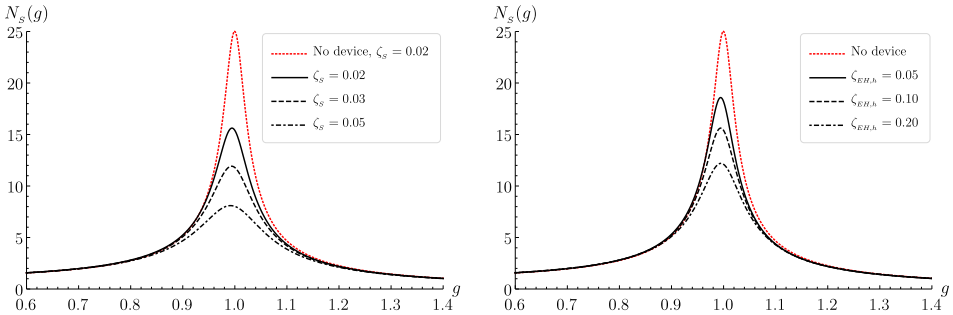

(a) $\zeta_{EH,h} = 0.10$, $\beta = 0.10$.

(b) $\zeta_S = 0.02$, $\beta = 0.10$.

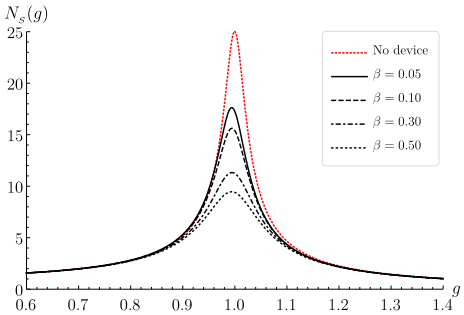

(c) $\zeta_S = 0.02$, $\zeta_{EH,h} = 0.10$.

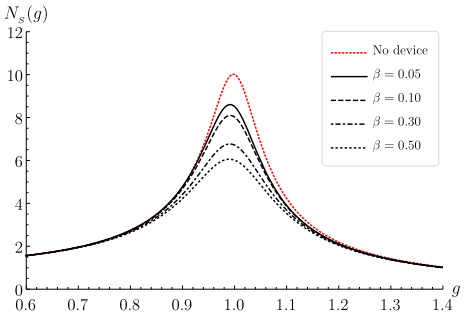

(d) $\zeta_S = 0.05$, $\zeta_{EH,h} = 0.10$.

Figure 2. Dynamic amplification factor $N_S(g)$ with $\mu = 0.01$, $\zeta_{EH,p} = 0.01$.

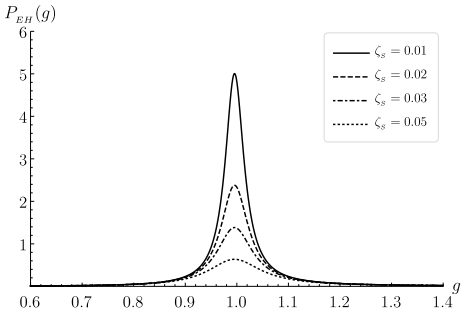

(a) $\zeta_{EH,h} = 0.10$, $\beta = 0.10$.

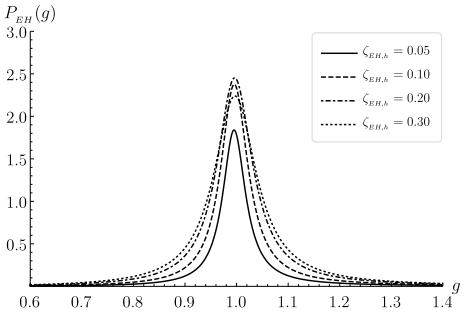

(b) $\zeta_S = 0.02$, $\beta = 0.10$.

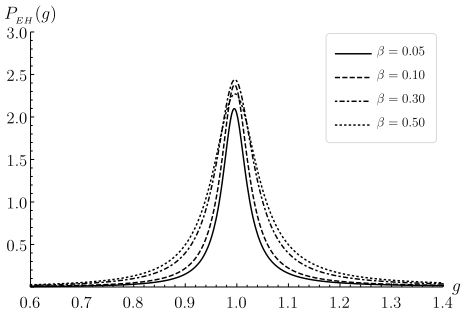

(c) $\zeta_S = 0.02$, $\zeta_{EH,h} = 0.10$.

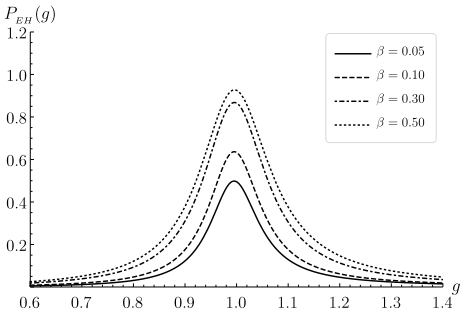

(d) $\zeta_S = 0.05$, $\zeta_{EH,h} = 0.10$.

Figure 3. Harvested energy $P_{EH}(g)$ with $\mu = 0.01$, $\zeta_{EH,p} = 0.01$.

The latter ratio needs to be doubled to achieve a reduction to the peak primary structure response of the order of 10%, while there is a clear trend of saturation to the reduction rate of the peak structural response at increasing ζ_{EH} values. More important, the dynamic amplification factor, plotted in Figs. 2c–2d for different inertance ratios, confirm that the EH-TMDI can perform significantly better as a vibration absorber as the inertance increases (with the TMDI stiffness and the damping ratio changing according to Eqs. (15)). Notably, the improvement in vibration suppression does not depend on the damping ratio of the primary structure (notice that the scale of the Y-axis differs in Figs. 2c–2d). Further, the rate of this improvement tends to lessen (saturate) for larger values of the inertance. These trends are similar to those observed for the TMDI (Fig. 1b) at increasing inertance (see for example [20] for the case of optimally-designed TMDI-equipped undamped SDOF structures under harmonic base excitation), and are further consistent with the improvements observed in vibration suppression for the case of the classical TMD (Fig. 1a) with increasing attached mass ratio [2]. In fact, a comparison between Figs. 2b and 2c suggests that the most influential property of the EH-TMDI that leverages its vibration suppression capabilities is the inertance ratio for a fixed mass ratio, rather than the damping coefficient of the EM.

Turning the attention to the potential energy harvesting capability of the EH-TMDI, it is seen in Fig. 3a that the damping of the primary structure has a detrimental effect: a small increase of ζ_S leads to a dramatic reduction of the available energy to be harvested, for fixed EH damping ratio ζ_{EH} and inertance ratio β. Furthermore, Fig. 3b suggests that, contrary to the level of vibration suppression for the primary structure, the amount of energy available for harvesting by the EM is strongly influenced by the operating damping ratio of the EM. In fact, the energy harvested at resonance increases by about 70% by doubling the damping ratio ζ_{EH}, and this trend does not saturate at increasing values of ζ_{EH}, while it applies for a relatively broad band of frequencies, within an interval $g = [0.9, 1.1]$. On the antipode, a comparison between Figs. 3c and 3d with Figs. 2c and 2d, respectively, evidences that the inertance ratio does not affect the energy harvesting potential of the EH-TMDI to the same extent as its vibration suppression capability. Still, it is important to note that the available energy to be harvested increases at increasing inertance ratio, despite a clear saturation trend for higher values of the inertance, and this occurs across a wide band of frequencies, that is, within at least an interval $g = [0.8, 1.2]$. Therefore, it appears that higher values of inertance benefits the performance of the EH-TMDI in terms of both vibration suppression and energy harvesting, a feature that is further discussed in the following section.

It is important to note that this is not the case with the commonly-considered TMD configurations for energy harvesting which replace the viscous damper in Fig. 1a by either a standard EM [11, 13] or piezoelectric material [14]. In these typical TMD-based configurations for energy harvesting, there appears to be a trade-off between energy harvesting potential and vibration suppression which is controlled by the attached mass: a larger attached mass yields better vibration absorption but reduces the available energy to be harvested, while smaller masses allows for larger amounts of energy to be harvested within a response cycle of oscillation but with the caveat of higher peak displacements of the primary mass. From a practical viewpoint, several comments are pertinent in view of the herein reported analytical data. First of all, it is noted that the primary structure damping ratio cannot normally vary in an arbitrary manner in practical applications as it is a fixed inherent property of the structural system to be controlled. However, the influence of this parameter on the amplitudes of the dynamic amplification factor in Eq. (13) and, more important, on the available energy to be harvested as quantified in Eq. (14), makes essential to have an accurate estimate of the rate of the inherent damping, to achieve a valid optimum design and to assess with accuracy the overall performance of the EH-TMDI. Contrary to the structural damping ratio, the EH damping ratio can vary at will as this depends on the properties of the EM and of the energy harvesting circuitry considered

to transform the kinetic energy to electric energy and store it [11, 13, 15]. In fact, ζ_{EH} varies during a structural response cycle when energy scavenging takes place, although, in the herein parametric analysis, an average value over a structural response cycle is assumed while the EM operates in a passive mode, which is a common assumption in the literature in undertaking analytical work to probe into the behaviour of TMDs and, more generally, of dynamic vibration absorbers with energy harvesting capabilities [13, 14].

Arguably, the critical property of the EH-TMDI that controls its performance both in terms of energy harvesting and vibration suppression is the inertance ratio, which can be set arbitrarily, without significant change of the overall weight of the EH-TMDI. For instance, in the case of flywheel-based inerters linked through gearing to ball-screw or rack and pinion mechanisms, the inertance can be changed by varying the gear ratio [16, 26]. A rather important feature of the herein proposed EH-TMDI, as already discussed, is the fact that by increasing the inertance ratio the available energy to be harvested increases, while the peak displacement response of the primary structure decreases, at least for the cases plotted in Figs. 2–3, and this happens within the same frequency band centred at the resonant frequency. This favourable attribute is further exploited in the following section to explore the potential of the EH-TMDI for simultaneous vibration suppression and energy harvesting in light of additional analytical results.

As a final practical remark, it is herein noted that the aforementioned vibration suppression and energy harvesting performance trends are not observed by any other alternative topology or assembly combining a classical TMD, an inerter, and an EM (all such possible topologies have been examined within a preliminary stage).

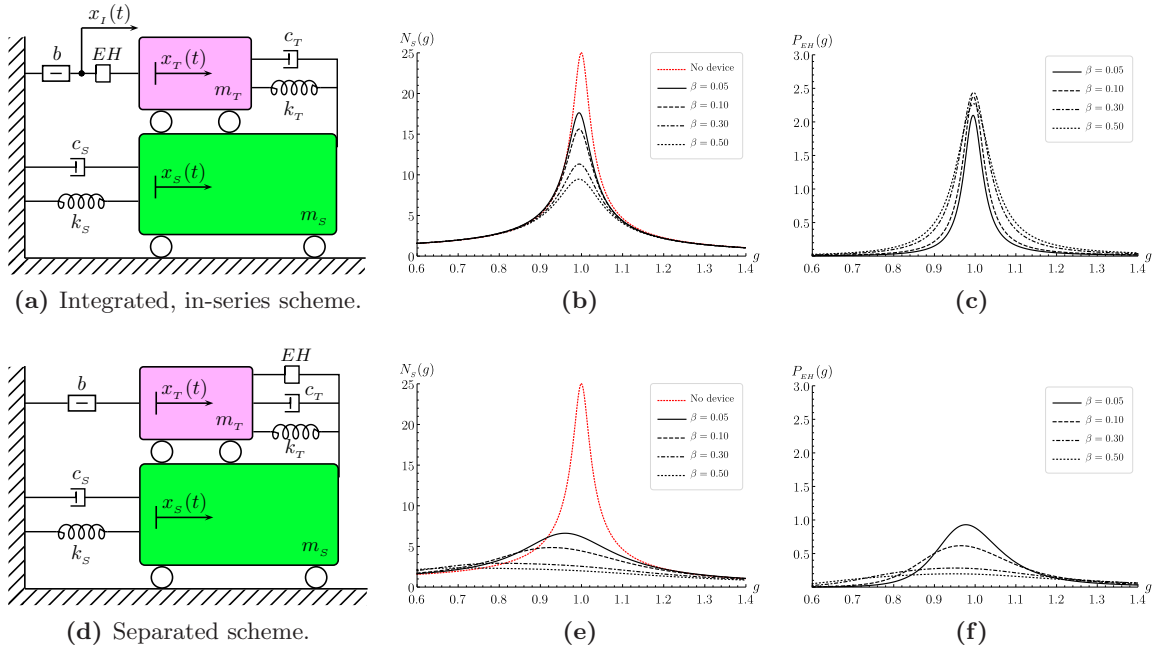

(a) Integrated, in-series scheme. **(b)** **(c)**

(d) Separated scheme. **(e)** **(f)**

Figure 4. Comparison between the (a)-(c) integrated, in-series layout and the (d)-(f) separated layout for the proposed EH-TMDI: topology ((a),(d)), dynamic amplification factor of the primary structure N_S ((b),(e)), harvested power P_{EH} ((c),(f)), with $\mu = 0.01$, $\zeta_{EH,p} = 0.01$, $\zeta_{EH,h} = 0.10$.

To further appreciate this issue, an example is shown in Fig. 4, where the available energy to be harvested and the dynamic amplification factor of the primary structure displacement obtained for the proposed EH-TMDI and for an alternative configuration previously considered

in the literature [21] are juxtaposed. Evidently, the alternative configuration (which actually coincides with the typical TMD-based configurations considered in the literature for energy harvested with the addition of an inerter linking the attached mass to the ground), does not share the advantages of the proposed EH-TMDI configuration in Fig. 1c. Larger inertance values do reduce significantly the peak amplitude of the primary structure displacement, but they also abate the available energy to be harvested, while the local maxima of the plotted curves move to the left of the resonant frequency and do not occur at the same frequency, in general. This renders the problem of optimum design for simultaneous vibration suppression and energy harvesting a challenging task.

5. Simultaneous vibration suppression and energy harvesting performance at resonance

It has been analytically verified in the previous section that, for the herein proposed EH-TMDI, the peak of available energy for harvesting purpose and the peak of vibration suppression occurs at the same (almost resonant) frequency $g = 1$, where vibration control performance becomes critical for harmonically-excited SDOF primary structures.

This observation allows for further exploring the influence of the inertance ratio β to the performance of the EH-TMDI for simultaneous vibration suppression and energy harvesting. This is done in Fig. 5, where the quantities in Eqs. (13)–(14) evaluated at resonance are plotted against the ratio of the inertance over the attached TMD mass $\delta = \beta/\mu$ [27] for two different values of attached mass ratios and structural damping ratios. In all cases, the effective damping ratio of the EM is fixed at $\zeta_{EH,h} = 0.1$. Note that all curves in the two panels of Fig. 5 are normalised to the global peak value attained by the same kind of curve for the two different attached mass ratios, to facilitate a comparison between the achieved level of vibration suppression and potential energy harvesting simultaneously at resonance.

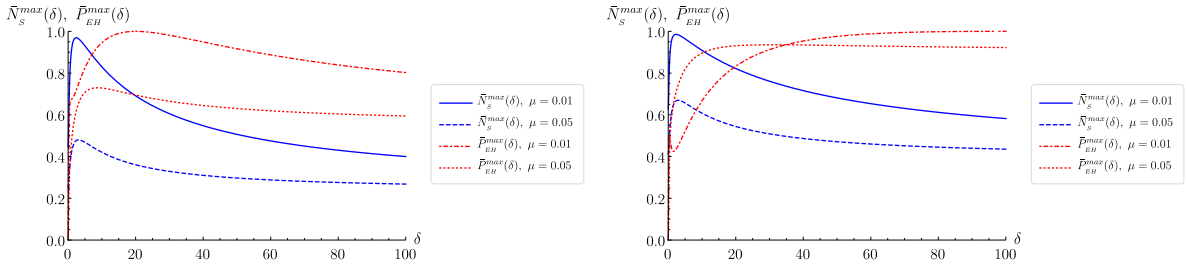

(a) $\zeta_S = 0.02$. **(b)** $\zeta_S = 0.05$.

Figure 5. Maximum dynamic amplification factor $N_S(\delta)$ and harvested power at resonance $P_{EH}(\delta)$ with $\zeta_{EH,p} = 0.01$, $\zeta_{EH,h} = 0.10$.

In all cases considered, it is seen that better vibration suppression is achieved beyond a value about $\delta > 2$. The latter can be interpreted as a sort of lower bound for the inertance value of practical interest in considering the EH-TMDI for simultaneous vibration suppression and energy harvesting. The rate of improvement of the vibration suppression is higher for a lower attached mass (i.e., an increase to the inertance is more effective for smaller attached TMD mass), though, better vibration suppression is achieved by the larger attached mass for the same value of δ. More important, it is seen that for the lightly damped primary structure ($\zeta_S = 2\%$, representative of bare steel/metal structures and structural components), better vibration suppression and energy harvesting is achieved as the inertance increases up to a critical value of $\beta = 0.2$ approximately, which is not significantly dependent on the attached mass. Above this critical value, the available

energy for harvesting at resonance negligibly reduces for the larger attached mass $\mu = 0.05$ and slightly more for the smaller attached mass, while increasingly better vibration suppression is achieved. Therefore, there is a well-defined range of inertance values that higher available energy to harvest and improved vibration suppression (at resonance) is achieved by increasing the inertance value. Further, from a design viewpoint, the value of the desired ratio δ will actually be dependent on the assigned weight of the two objectives (vibration suppression and harvested energy).

Notably, for the case of higher damped primary structures ($\zeta_S = 5\%$, representative of reinforced concrete building structures with infill walls), better vibration suppression and energy harvesting are monotonically attained at increasing inertance, though a clear saturation trend to the improvement of both objectives is observed for larger β, which is more significant for the case of the larger attached mass.

6. Concluding remarks

A novel configuration for simultaneous vibration suppression and energy harvesting in harmonically-excited structures modelled as damped SDOF dynamical systems has been introduced in this paper, termed energy harvesting-enabled tuned mass-damper-inerter (EH-TMDI). The EH-TMDI comprises a classical linear TMD "skyhooked" by an electromagnetic (EM) energy harvester connected in series with a grounded inerter.

Through comprehensive parametric analyses focusing solely on the mechanical domain, it has been demonstrated that by varying the inertial constant of the inerter (inertance) and by adjusting the stiffness and damping properties of the TMD by means of simple design formulae, enhanced vibration suppression (in terms of peak displacement of the SDOF primary structure) and energy harvesting (in terms of relative velocity at the terminals of the EM) may be achieved simultaneously at near-resonance frequencies for a fixed attached TMD mass. This is not the case with the commonly-considered in the literature TMD-based energy harvesters, for which a stringent trade-off exists between vibration suppression and energy harvesting. Furthermore, it has been shown in the considered parametric analyses that the damping of the primary structure influences significantly the available energy to be harvested.

Therefore, the inherent structural damping should not be ignored for the sake of facilitating optimum design, and attention should be paid on estimating its value with good accuracy, by using standard system identification techniques in practical applications. Moreover, it was found that the effective value of the damping ratio of the EM, assumed to be constant in the analysis, influences more the vibration suppression performance of the EH-TMDI than the available energy to be harvested.

Overall, the herein reported analytical data and parametric analyses points to the fact that the proposed EH-TMDI is amenable to a meaningful multi-objective optimum design procedure, which is left for future work.

Acknowledgements

This research work is funded by the *"Engineering and Physical Sciences Research Council (EPSRC)"* (Project Reference EP/M017621/1), UK, 2015–2016. The Authors are grateful for this financial support.

References

[1] Frahm H. *Device for damping vibrations of bodies*, U.S. Patent No. 989958, pp. 3576–3580, 1911.

[2] Den Hartog JP. *Mechanical Vibrations*, McGraw-Hill, 4th ed., 1956.

[3] Salvi J, Rizzi E. Closed-form optimum tuning formulas for passive Tuned Mass Dampers under benchmark excitations, *Smart Structures and Systems*, doi: 10.12989/sss.2016.17.2.231, 17(2):231–256, 2016.

[4] Asami T, Nishihara O, Baz AM. Analytical solutions to H_∞ and H_2 optimization of dynamic vibration absorber attached to damped linear systems, *Journal of Vibrations and Acoustics, ASME*, 124(2):284–295, 2002.

[5] Krenk S. Frequency Analysis of the Tuned Mass Damper, *Journal of Applied Mechanics (ASME)*, 72(6):936–942, 2005.

[6] Bakre SV, Jangid RS. Optimum parameters of tuned mass damper for damped main system, *Structural Control and Health Monitoring*, 14(3):448–470, 2006.

[7] Salvi J, Rizzi E. Optimum tuning of Tuned Mass Dampers for frame structures under earthquake excitation, *Structural Control and Health Monitoring*, doi: 10.1002/stc.1710, 22(4):707–725, 2015.

[8] Salvi J, Rizzi E, Rustighi E, Ferguson NS. On the optimisation of a hybrid Tuned Mass Damper for impulse loading, *Smart Materials and Structures*, doi:10.1088/0964-1726/24/8/085010, 24(8)(2015)085010, 15 pages, 2015.

[9] Cassidy IL, Scruggs JT, Behrens S, Gavin HP. Design and experimental characterization of an electromagnetic transducer for large-scale vibratory energy harvesting applications, *Journal of Intelligent Material Systems and Structures*, 22(17):2009–2024, 2011.

[10] Shen W, Zhu S, Xu Y, An experimental study on self-powered vibration control and monitoring system using electromagnetic TMD and wireless sensors, *Sensors and Actuators A: Physical*, 180:166-176, 2012.

[11] Tang X, Zuo L. Simultaneous energy harvesting and vibration control of structures with tuned mass dampers, *Journal of Intelligent Materials Systems and Structures*, 23(18):2117–2127, 2012.

[12] Zuo L, Tang X. Large-scale vibration energy harvesting, *Journal of Intelligent Materials Systems and Structures*, 24(11):1405–1430, 2013.

[13] Gonzalez-Buelga A, Clare LR, Cammarano A, Neild SA, Burrow SG, Inman DJ. An optimised tuned mass damper/harvester device, *Structural Control and Health Monitoring*, 21(8):1154–1169, 2014.

[14] Adhikari S, Ali F. Energy Harvesting Dynamic Vibration Absorbers, *Journal of Applied Mechanics* (ASME), 80(4):041004-1, 9 pages, 2013.

[15] Zhu S, Shen WA, Xu Y-L. Linear electromagnetic devices for vibration damping and energy harvesting: modeling and testing, *Engineering Structures*, 34:198–212, 2012.

[16] Smith MC. Synthesis of Mechanical Networks: the Inerter, *IEEE Transactions on Automatic Control*, 47(10):1648–1662, 2002.

[17] Aldraihem O, Baz A. Energy Harvester with a Dynamic Magnifier, *Journal of Intelligent Materials Systems and Structures*, 22(6):521–530, 2011.

[18] Tang X, Zuo L. Enhanced vibration energy harvesting using dual-mass system, *Journal of Sound and Vibration*, 330(21):5199–5209, 2011.

[19] Marian L, Giaralis A. Optimal design of inerter devices combined with TMDs for vibration control of buildings exposed to stochastic seismic excitations, Proceedings the 11th International Conference on Structural Safety and Reliability for Integrating Structural Analysis, Risk and Reliability (ICOSSAR 2013), New York, US, 16–20 June 2013, 8 pages, 2013.

[20] Marian L, Giaralis A. Optimal design of a novel tuned mass-damper-inerter (TMDI) passive vibration control configuration for stochastically support-excited structural systems, *Probabilistic Engineering Mechanics*, 38:156–164, 2014.

[21] Marian L, Giaralis A. Vibration suppression and energy harvesting in tuned-mass-damper-inerter (TMDI) equipped harmonically support-excited systems, Proceedings of the 6th World Conference on Structural Control and Monitoring, 15–17 July 2014, Barcelona, Spain, 2014.

[22] Scruggs JT, Iwan WD. Control of a Civil Structure Using an Electric Machine with Semiactive Capability, *Journal of Structural Engineering* (ASCE), 129(7):951–959, 2003.

[23] Palomera-Arias R, Connor JJ, Ochsendorf JA. Feasibility Study of Passive Electromagnetic Damping Systems, *Journal of Structural Engineering* (ASCE), 134(1):164–170, 2008.

[24] Di Monaco F, Ghandchi Tehrani M, Elliott SJ, Bonisoli E, Tornincasa S. Energy harvesting using semi-active control, *Journal of Sound and Vibration*, 332(23):6033–6043, 2013.

[25] Zilletti M, Elliott SJ, Rustighi E. Optimisation of dynamic vibration absorbers to minimise kinetic energy and maximise internal power dissipation, *Journal of Sound and Vibration*, 331(18):4093–4100, 2012.

[26] Papageorgiou C, Smith MC. Laboratory experimental testing of Inerters, Proceedings of the 44th IEEE Conference on Decision and Control and European Control Conference, Seville, Spain, 12–15 December 2005, 6 pages, 2005.

[27] Hu Y, Chen MZQ. Performance evaluation for inerter-based dynamic vibration absorbers, *International Journal of Mechanical Sciences*, 99:297–307, 2015.